Structure of the amorphous phase in highly drawn poly(vinyl alcohol) fibres

Po-Da Hong*
Department of Textile Engineering, National Taiwan Institute of Technology, Taipei 106, Taiwan

and Keizo Miyasaka
Department of Organic and Polymeric Materials, Tokyo Institute of Technology, Meguro-ku, Tokyo 152, Japan
(Received 13 May 1992; revised 4 March 1993)

Wide-angle X-ray diffraction analysis of poly(vinyl alcohol) (PVA) fibres shows that the amorphous scattering at $2\theta = 20°$ concentrates on the equator, and the degree of concentration becomes stronger with increasing draw ratio. This indicates that the amorphous chains must be highly oriented in the highly drawn fibres. Small-angle X-ray scattering (SAXS) analysis shows that the meridional SAXS intensity of the highly drawn fibres decreases with increasing draw ratio, indicating that the amorphous chains are packed more densely. On the other hand, a new meridional diffraction peak appears at $2\theta = 35.5°$ ($d = 2.52$ Å) and the intensity becomes stronger with increasing draw ratio. The $2\theta = 35.5°$ diffraction peak is broader than the (020) diffraction ($d = 1.26$ Å) peak. The thermal expansion coefficient estimated from the $2\theta = 35.5°$ peak is positive, while that estimated from the (020) peak is negative above ca. 120°C. These results suggest that this meridional peak ($2\theta = 35.5°$) is not the (010) diffraction, which never appears in the normal PVA crystal but might appear in some disordered crystals, but is due to the intrachain scattering of a single amorphous chain with an almost planar zigzag conformation.

(Keywords: X-ray diffraction; poly(vinyl alcohol) fibre; amorphous scattering)

INTRODUCTION

It is well known that the X-ray diffraction patterns of most amorphous polymers have one or two amorphous haloes due to interchain and intrachain interferences. Uniaxial drawing of amorphous polymers such as polystyrene (PS)[1] and poly(methyl methacrylate) (PMMA)[2] sometimes makes these amorphous scatterings concentrate on the equator or the meridian, respectively, indicating that amorphous chains orient to the drawing direction. In the case of semicrystalline polymers, how the structure of the amorphous phase depends on the sample preparation method is a comparatively difficult but very important subject which attracts our interest.

Recently, many authors have used profile-fitting procedures in evaluating the amorphous scatterings in the X-ray diffraction patterns of semicrystalline polymers such as nylon-6[3-5], poly(ethylene terephthalate) (PET)[6] and poly(vinyl chloride) (PVC)[7]. In our previous study[8], a new evaluation method for the meridional amorphous scattering of α-form nylon-6 fibres was proposed, and the result showed that the meridional amorphous scattering ($2\theta = 20.45°$, $d = 4.3$ Å) concentrates on the meridian under uniaxial extension. This result suggests that the amorphous scattering may be due to intrachain interference, i.e. the amide groups of a single chain in the amorphous phase. On the other hand, Murthy *et al.*[9] reported that the distribution of the amorphous scattering at $2\theta = 21°$ is anisotropic and concentrates on the equator for nylon-6 fibres. These results in nylon-6 fibres indicate that the amorphous scattering peak at $2\theta = 21°$ may comprise contributions from both interchain and intrachain scatterings.

In this study, a meridional diffraction at $2\theta = 35.5°$ ($d = 2.52$ Å) appeared in highly drawn PVA fibres which has not been observed in ordinary PVA fibres or highly drawn PE fibres. The identity of this meridional diffraction and the change in structure of the amorphous phase with drawing in highly drawn PVA fibres were investigated. Although the backbone structures of nylon-6 and poly(vinyl alcohol) (PVA) chains are similar to that of polyethylene (PE), the first two have amide and hydroxy groups, respectively, in place of the hydrogen atoms in PE. On the other hand, these crystalline polymers have a common amorphous scattering peak at $2\theta = 20°$ corresponding to interchain interference in the amorphous phase. As to the crystal structures, both PE and PVA crystals are composed of pairs of chains packed in each unit cell. Both of them have the same repeat distance (ca. 2.52 Å)[10,11] corresponding to the chemical unit of a planar zigzag carbon chain. In spite of the fibre period of 2.52 Å, the meridional crystal diffraction only appears at $2\theta = 75°$ ($d = 1.26$ Å) on the meridian for both PE and PVA. In the case of PVA, two chains are packed with a phase difference of half the repeat distance in the crystal, while in the case of PE the repeat distance of the CH_2 along the chain axis is half the real repeat distance corresponding to the chemical unit. The (001)

* To whom correspondence should be addressed

0032-3861/94/07/1369-06

structure factor in the PE crystal and the (010) structure factor in the PVA crystal must both be zero, i.e. no $d = 2.52$ Å meridional diffraction appears in these crystals. On the other hand, the structure factor of a single chain, which may be considered to be a one-dimensional crystal, is still zero in (001) of the PE chain but not in (010) of the PVA chain because of the difference in the molecular structures. If the highly extended and oriented amorphous chains really exist in the amorphous phase of highly drawn samples, the difference in the molecular structure between PE and PVA must give rise to the different meridional diffractions.

EXPERIMENTAL

Highly oriented PVA fibres (Kuraray Co. Ltd, Japan) were used as samples. The spinning conditions were as shown in *Table 1*. The as-spun fibre (no. 1) was prepared by a one-stage wet drawing, while the highly drawn fibres (nos 2 to 4) were prepared by a two-stage drawing, i.e. a second-stage dry drawing after the same drawing as that for no. 1 fibre; in other words, nos 2 to 4 fibres were obtained by further drawing of no. 1 fibre. It should be noted that the highly drawn fibres used in this study had high modulus and high strength compared to the commercial PVA fibres prepared by the conventional method. The fibres were aligned as parallel as possible to make a plate-shaped specimen about 1 mm in thickness, and then fixed to a stainless steel holder for the X-ray measurements.

Wide-angle X-ray diffraction (WAXD) photographs were taken by a flat camera with Ni-filtered CuKα radiation from a Rigaku XG working at 35 kV and 20 mA. The WAXD intensity was measured with graphite-monochromatized CuKα radiation (wavelength 1.54 Å) generated at 50 kV and 180 mA in a Rigaku Rota Flex RU200, using a scintillation counter with a pulse height analyser. WAXD intensity curves obtained at a scanning speed of 0.5° min^{-1} were corrected for air scattering and standardized by quantity of sample. The instrumental broadening was corrected using silicon powder as a standard material. The crystallite orientation function f_c was evaluated by azimuthal scanning of the (020) diffraction (the crystal is monoclinic and the chain axis is parallel to the b axis) at a scanning speed of 2° min^{-1}. The crystallite thickness was estimated from the integral breadth of the (020) diffraction using the Scherrer equation[12,13]. The long spacing was evaluated from the scattering angle of the small-angle X-ray scattering (SAXS) meridional maximum.

RESULTS AND DISCUSSION

Figures 1a and *1b* show WAXD photographs of the as-spun fibre (no. 1) and a highly drawn fibre (no. 2), respectively. These photographs indicate that the two-stage drawing increases the degree of crystallite orientation. In order to investigate the effect of drawing on the crystallinity, the azimuthally averaged intensity curves of the fibres were measured with the results shown

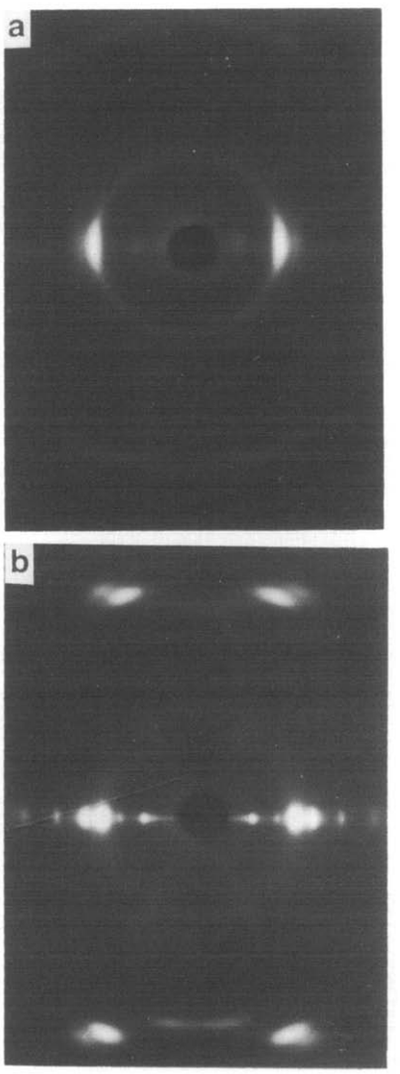

Figure 1 WAXD photographs of PVA fibres: (a) as-spun fibre (no. 1); (b) highly drawn fibre (no. 2)

Table 1 Spinning conditions of the PVA fibres studied

Sample no.	DP^a	Solvent	First-stage (wet) drawing	Second-stage (dry) drawing		Total draw ratio	Fineness of fibre (denier)
				Temperature (°C)	Ratio		
1	8800	DMSO	4×	–	1×	4.0×	13.98
2	8800	DMSO	4×	245	3.5×	14.0×	3.75
3	8800	DMSO	4×	245	4.25×	17.0×	3.06
4	8800	DMSO	4×	250	4.95×	19.8×	2.63

[a] Degree of polymerization

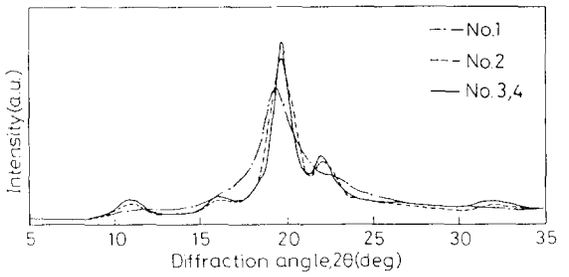

Figure 2 Azimuthally averaged intensity curves of the PVA fibres

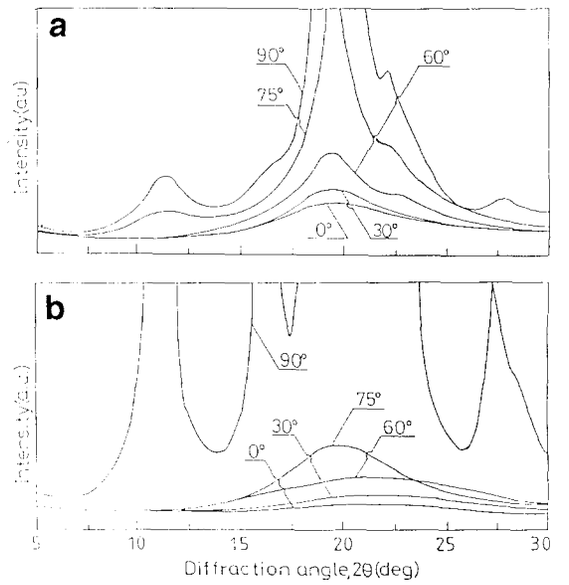

Figure 3 A series of 2θ scanning intensity curves at different azimuthal angles ϕ, where $\phi = 0°$ and 90° represent the meridian and equator, respectively: (a) as-spun fibre (no. 1); (b) highly drawn fibre (no. 4)

in *Figure 2*. In measuring these curves, the fibres were rotated quickly in the plane normal to the incident beam, using a Rigaku rotating apparatus, to eliminate the molecular orientation effect. *Figure 2* shows that the intensity curves of nos 2 to 4 fibres are much sharper than that of no. 1 fibre, indicating that the second-stage drawing increases the crystallinity. On the other hand, no remarkable difference is observed among the curves of the highly drawn (nos 2 to 4) fibres, implying no noticeable difference in the crystallinity among these fibres. In other words, nos 2 to 4 fibres have nearly the same fraction of the amorphous phase.

As mentioned earlier, PVA shows an amorphous scattering peak at $2\theta = 20°$ due to interchain interference, as does PE. Thus, any structural change in the amorphous phase, if it happens, may be indicated by a change in this ($2\theta = 20°$) scattering. *Figures 3a* and *3b* show the 2θ scanning intensity curves of the as-spun (no. 1) fibre and a highly drawn (no. 4) fibre, respectively, as a function of the azimuthal angle ϕ, where $\phi = 0°$ and 90° represent the meridian and equator, respectively. Because of the low degree of crystallite orientation, the amorphous scattering curve of the as-spun (no. 1) fibre is overlapped by crystalline scattering above $\phi = 60°$, while in the case of the highly drawn (no. 4) fibre this occurs above $\phi = 75°$. In the highly drawn fibres, the shape of the amorphous scattering 2θ scanning curve varies depending on ϕ: the amorphous scattering profile becomes much narrower and more symmetrical, and the amorphous scattering intensity increases with increasing ϕ towards the equator. A similar result has been observed in nylon-6 fibres by Murthy *et al.*[9]. Although the amorphous scattering profile on the equator is difficult to determine, the increase in the amorphous scattering intensity with ϕ indicates that the amorphous scattering concentrates on the equator for all fibre specimens.

Figure 4 shows the azimuthal distribution curves of the peak intensity at $2\theta = 20°$ for all fibres. Comparison of these curves indicates that the rate of increase of the peak intensity with increasing ϕ is somewhat different among them, i.e. the rate of increase rises with increasing draw ratio. This implies that the degree of orientation of the amorphous chains increases with drawing. These results and those discussed earlier suggest that the aggregation of oriented and extended chains occurs in the amorphous phase.

Figure 5 shows the changes in the meridional SAXS curves with drawing. Comparison of no. 1 and no. 2 fibres shows that the second-stage drawing causes the peak due to the long spacing to shift to the small angle side and the peak intensity to increase remarkably. This means that the long spacing and the degree of orientation increase remarkably with the second-stage drawing. On the other hand, the results for the highly drawn fibres (nos 2 to 4) show that the peak weakens and becomes broader with drawing, while these specimens have almost the same degree of crystallite orientation, as shown in

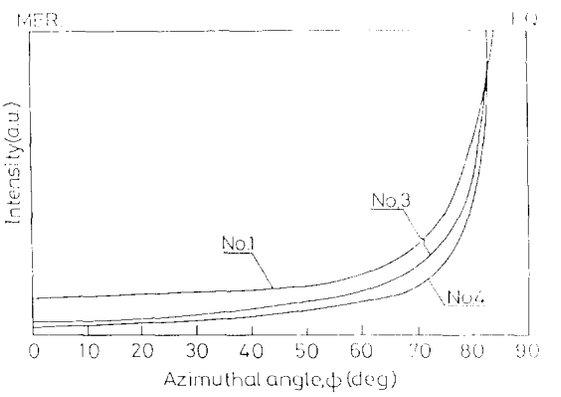

Figure 4 The azimuthal profiles of the peak intensity at $2\theta = 20°$ for the PVA fibres

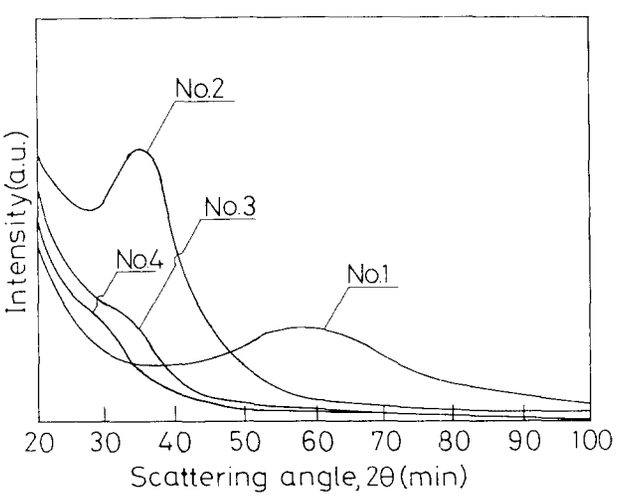

Figure 5 Meridional SAXS intensity curves of the PVA fibres

Table 2 Tensile properties and structure parameters of the PVA fibres

Sample no.	Total draw ratio	Tensile modulus (GPa)	Tensile modulus ($g\,d^{-1}$)	Tensile strength (GPa)	Tensile strength ($g\,d^{-1}$)	Breaking strain (%)	f_c[a]	D_{020}[b] (Å)	L[c] (Å)
1	4.0	6.3	55	0.4	3.0	59.0	0.856	34	85
2	14.0	41.8	364	2.0	17.6	5.2	0.982	102	160
3	17.0	49.1	428	2.3	19.9	4.4	0.986	116	178
4	19.8	54.4	474	2.5	20.8	3.9	0.988	121	182

[a] Crystallite orientation
[b] Crystallite size estimated from the (020) profile
[c] Long spacing

Table 2. The peak still remains even at the highest draw ratio, indicating that the fibre still has a serial crystalline–amorphous structure. Since the SAXS peak intensity is proportional to the square of the density difference between the crystalline and amorphous phases, the result in *Figure 5* indicates that the density difference tends to decrease with drawing, which is mainly due to the increase in density of the amorphous phase. This suggests that the amorphous chains must become more densely packed with increasing draw ratio during the second-stage drawing.

Table 2 shows the tensile properties and structure parameters of the PVA fibre specimens. Although the orientation function f_c, crystallite thickness D_{020} and long spacing L increase very much with draw ratio, the differences in these structure parameters are not very remarkable between the more highly drawn fibres (nos 3 and 4). Combination of these results with those mentioned above indicates that the increase in the tensile properties in the highly drawn fibres is mainly due to a change in the amorphous structure, i.e. the amorphous chains become more densely packed and oriented with drawing. Wu *et al.*[14] have already widely and systematically discussed the correlation between the tensile properties and morphological changes in drawn PE fibres. They also suggested that, for many specimens prepared by different spinning conditions, the meridional SAXS intensity is found to correlate better with the tensile strength and modulus of drawn PE fibres than any other structural parameter, such as crystallite dimensions and orientation function. The enhancement of mechanical properties in highly drawn samples must mainly relate to the structural changes in the amorphous phase.

Figure 6 shows the meridional intensity curves of the fibre specimens. The broad peak at $2\theta = 20°$ is due to the interchain scattering of the amorphous phase. On the other hand, the meridional peak at $2\theta = 75°$ ($d = 1.26$ Å) is well known to be due to the (020) diffraction, and becomes much sharper and more intense with drawing. These changes correspond to the increases in crystallite thickness and degree of orientation shown in *Table 2*. Besides these two peaks, the as-spun (no. 1) fibre has two meridional diffraction peaks at $2\theta = 37°$ and 41°, and they are the (110) and (111), (11$\bar{1}$) diffractions, respectively. Because of the low degree of crystallite orientation, these diffractions have drifted into the meridian. The highly drawn (nos 2 to 4) fibres show a new peak at $2\theta = 35.5°$ ($d = 2.52$ Å) which becomes stronger with increasing draw ratio. It should be noted that no one, for example Sakurada *et al.*[15], has reported this meridional diffraction for highly oriented, ordinary PVA fibres.

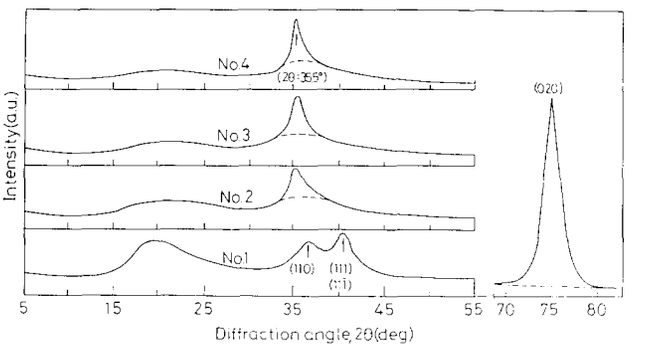

Figure 6 Meridional X-ray diffraction intensity curves of the PVA fibres. The dashed lines represent the amorphous scattering background assumed for evaluating the integral breadths ΔS

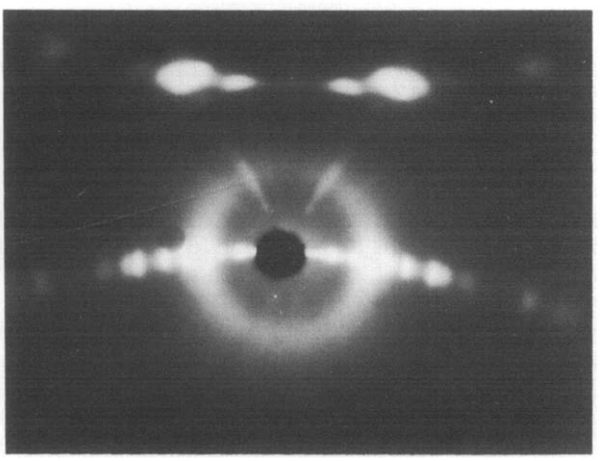

Figure 7 A titled-fibre WAXD photograph of a highly drawn PVA fibre (no. 4), where the angle between the fibre axis and the incident X-ray beam was 72°

Figure 7 shows a titled-fibre WAXD photograph of a highly drawn fibre (no. 4), where the angle between the fibre axis and the incident X-ray beam is 72°. On the first-layer line, the off-meridian diffractions are the (110) and (111), (11$\bar{1}$) diffractions, respectively. Besides these diffraction spots, a diffuse, layer-shaped diffraction corresponding to $2\theta = 35.5°$ on the meridian is observed. It should be noted that a same titled-fibre WAXD photograph of PE[16] has not shown any meridional diffraction on the first-layer line. The identification of this meridional diffraction at $2\theta = 35.5°$ in highly drawn PVA fibres is the most important part of this study.

Here, we first assume that this meridional peak is due to the (010) diffraction of the PVA crystal (named

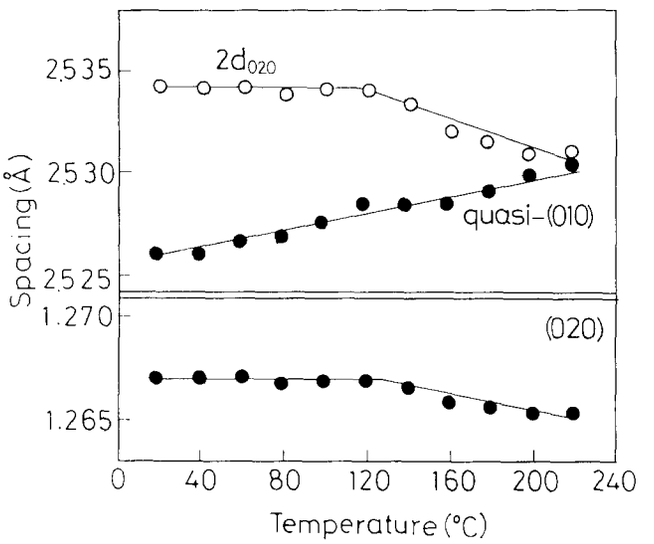

Figure 8 Variations in the quasi-(010) and (020) spacings of the PVA crystal with temperature. Also plotted is the variation in $2d_{020}$ with temperature

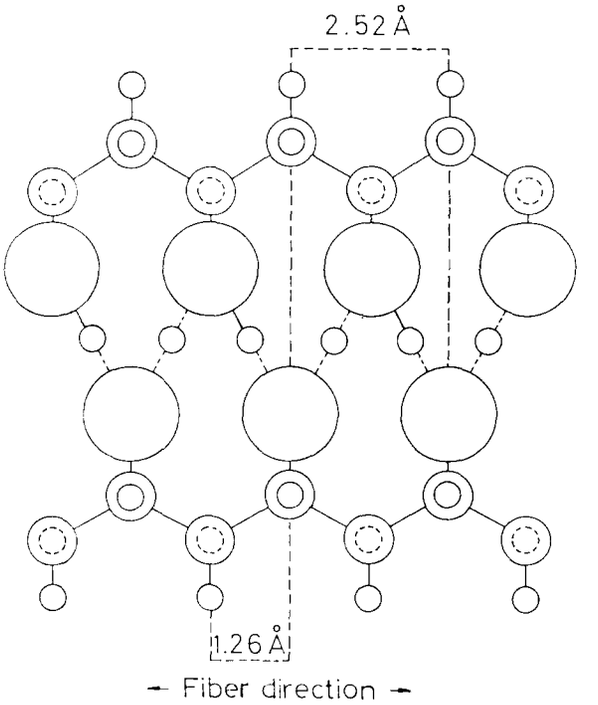

Figure 9 A schematic figure of the PVA crystal as proposed by Mooney[22] where the PVA chains are projected on the (101) plane. The circles in descending order of size represent oxygen, carbon and hydrogen atoms, respectively. The dashed and solid circles distinguish between hydrogen atoms on opposite sides of the chains

quasi-(010)), because its spacing is about twice that of (020). As mentioned earlier, the (010) diffraction should not appear for the PVA crystal. However, there is a possibility that some of the lattice distortions relating to the phase between the neighbouring chains might make this diffraction appear. Under this consideration, the integral breadths ΔS were evaluated to check whether or not these two diffractions are related as first-order and second-order reflections. Although the exact ΔS_{010} is difficult to estimate, a reasonable breadth for this diffraction was evaluated using the background shown by the dashed lines in *Figure 6*. The values of ΔS_{010} are in the range $13.0–16.8 \times 10^{-3}$ Å^{-1}, while those of ΔS_{020} are in the range $8.2–9.8 \times 10^{-3}$ Å^{-1} for highly drawn (nos 2 to 4) fibres. The values of ΔS_{010} for all the highly drawn fibres are much larger than those of ΔS_{020}.

Figure 8 shows the temperature variations in the spacings of the quasi-(010) and (020) for a highly drawn (no. 4) fibre. It is well known that the thermal expansion of the PVA crystal lattice changes discontinuously at about 120°C[17,18], and that the crystallite has a second-order transition point at this temperature. *Figure 8* illustrates that the spacing of the (020) shows a deflection point due to the second-order transition at ca. 120°C and then decreases with increasing temperature above 120°C, while that of the quasi-(010) increases continuously with increasing temperature without any deflection point. In other words, the thermal expansion of the quasi-(010) is positive while that of the (020) is negative at high temperatures.

These results indicate that these two meridional diffractions are not related as first-order and second-order reflections. Accordingly, the meridional diffraction at $2\theta = 35.5°$ is considered not to be from the (010) diffraction of the PVA crystal but from highly oriented amorphous chains, i.e. highly extended tie chains. In a serial crystalline–amorphous, two-phase structure, the existence of highly extended tie chains in the amorphous phase is usually considered and suggested by many authors[19–21] for highly drawn samples. A highly extended tie chain may be considered as a one-dimensional crystallite which may make a sharp diffraction appear on the meridian, although the intensity will be much weaker than that of the crystallite diffraction.

A schematic model of the PVA crystal proposed by Mooney[22] is illustrated in *Figure 9*, which shows a pair of vinyl alcohol chains projected on the (101) plane and held together with a phase difference of 1.26 Å by hydrogen bonds. The 1.26 Å period will produce a very sharp and intense diffraction peak on the meridian for highly oriented and drawn samples. On the other hand, a single chain which has a planar zigzag conformation with glycol units in the 1,3 positions may make a diffraction appear on the meridian if the chain is highly extended or oriented. Under these considerations, we may understand the reason why this diffraction ($d = 2.52$ Å) appears on the meridian in PVA but not in PE for the same highly drawn sample. These considerations may be supported by the results from other oriented amorphous polymers such as PS[1] and PMMA[2] which also show an intrachain scattering on the meridian, although the chain conformations are different from that of PVA.

From the experimental results, the positive thermal expansion of the diffraction at $2\theta = 35.5°$ implies that the conformation of the tie chain is not complete but almost planar zigzag, because the thermal expansion coefficient is comparatively small (ca. 2×10^{-5} K^{-1}) and the spacing is almost twice that of the (020), as shown in *Figure 8*. However, as shown in *Figure 6*, an asymmetric profile of the meridional diffraction at $2\theta = 35.5°$ indicates that this profile may be composed of many components with a wide span of chain repeat distances shorter than that of the planar zigzag conformation. It is doubtful that the rate of extension of the amorphous chains should be uniform so that all of them may take the complete zigzag conformation. The appearance of this meridional diffraction is one of the unique characteristics of the structure of high-modulus, high-strength PVA fibres prepared by high drawing.

CONCLUSIONS

In this study, the structure of the amorphous phase was investigated by X-ray analysis for highly drawn PVA fibres. The results indicate that the amorphous scattering at $2\theta = 20°$ due to interchain interference concentrates on the equator, and that the amorphous chains must be packed more densely and oriented in highly drawn PVA fibres. This is why the tensile properties increase with high drawing, whereas the structural parameters such as crystallite size and degree of orientation show no remarkable changes in these highly drawn PVA fibres. On the other hand, a new meridional diffraction at $2\theta = 35.5°$ ($d = 2.52$ Å) appears for these highly drawn fibres. This diffraction is not considered to be from the (010) of the disordered PVA crystal but from the intrachain interference between the hydroxy groups of highly extended amorphous chains with almost planar zigzag conformations. The appearance of this meridional diffraction is one of the unique characteristics of the structure of high-modulus, high-strength PVA fibres prepared by high drawing.

REFERENCES

1 Williams, J. L., Karam, H. J., Cleereman, K. J. and Rinn, H. W. *J. Polym. Sci.* 1952, **8**, 245
2 Pick, M., Lovell, R. and Windle, A. H. *Polymer* 1980, **21**, 1017
3 Murthy, N. S. and Minor, H. *Polymer* 1990, **31**, 996
4 Gurato, G., Fichera, A., Grandi, F. Z., Zannetti, R. and Gannal, P. *Makromol. Chem.* 1974, **175**, 953
5 Heuvel, H. M. and Huisman, R. *J. Polym. Sci., Polym. Phys. Edn* 1981, **19**, 121
6 Murthy, N. S., Correale, S. T. and Minor, H. *Macromolecules* 1991, **24**, 1185
7 Guerrero, S. J., Veloso, H. and Randon, E. *Polymer* 1990, **31**, 1615
8 Hong, P. D. and Miyasaka, K. *Polymer* 1992, **33**, 3828
9 Murthy, N. S., Correale, S. T. and Moore, R. A. F. *J. Appl. Polym. Sci., Appl. Polym. Symp.* 1991, **47**, 185
10 Bunn, C. W. *Trans. Faraday Soc.* 1939, **35**, 482
11 Bunn, C. W. *Nature* 1948, **161**, 929
12 Bragg, W. L., James, R. and Bosanquet, W. *Philos. Mag.* 1921, **41**, 309
13 Bragg, W. L., James, R. and Bosanquet, W. *Philos. Mag.* 1921, **42**, 1
14 Wu, W., Simpson, P. G. and Black, W. B. *J. Polym. Sci., Polym. Phys. Edn* 1980, **18**, 751
15 Sakurada, I., Nukushima, Y. and Mori, N. *Kobunshikagaku* 1955, **12**, 307
16 Alexander, L. E. 'X-ray Diffraction Methods in Polymer Science', Wiley-Interscience, New York, 1969, p. 201
17 Shirakashi, K., Ishikawa, K. and Miyasaka, K. *Kobunshikagaku* 1964, **21**, 588
18 Hong, P. D. and Miyasaka, K. *Polymer* 1991, **32**, 3140
19 Peterlin, A. *J. Polym. Sci. (A-2)* 1969, **8**, 1151
20 Gibson, A. G., Davies, G. R. and Ward, I. M. *Polymer* 1978, **19**, 683
21 Zachariades, A. E. and Kanamoto, T. *J. Appl. Polym. Sci.* 1988, **35**, 1265
22 Mooney, R. C. L. *J. Am. Chem. Soc.* 1941, **63**, 2828